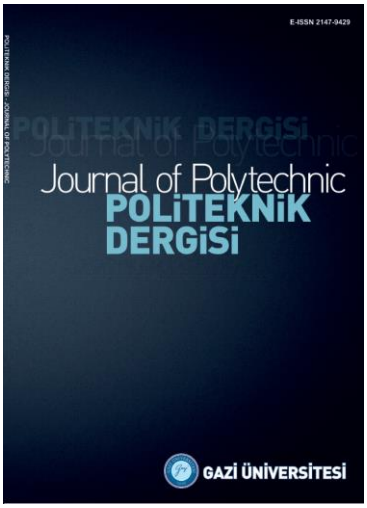

POLİTEKNİK DERGİSİ

JOURNAL of POLYTECHNIC

ISSN: 1302-0900 (PRINT), ISSN: 2147-9429 (ONLINE)
URL: http://dergipark.org.tr/politeknik

Experimental study on magnetorheological damper prototype and obtaining its equivalent damping coefficients

Manyetoreolojik amortisör prototipinin deneysel çalışması ve eşdeğer sönüm katsayılarının elde edilmesi

Yazar(lar) (Author(s)): *Turgay ERGİN[1], Duran ALTIPARMAK[2]*

ORCID[1]: 0000-0002-6396-1277

ORCID[2]: 0000-0002-8597-7923

To cite to this article: Ergin T. and Altıparmak D., "Experimental study on magnetorheological damper prototype and obtaining its equivalent damping coefficients", ***Journal of Polytechnic***, 26(2): 863-870, (2023).

Bu makaleye şu şekilde atıfta bulunabilirsiniz: Ergin T. and Altıparmak D., "Experimental study on magnetorheological damper prototype and obtaining its equivalent damping coefficients", ***Politeknik Dergisi***, 26(2): 863-870, (2023).

Erişim linki (To link to this article): http://dergipark.org.tr/politeknik/archive

DOI: 10.2339/politeknik.1078651

Experimental Study on Magnetorheological Damper Prototype and Obtaining Its Equivalent Damping Coefficients

Highlights

- *A prototype of the MR damper was designed, manufactured and tested.*
- *The equivalent damping coefficients of the MR damper were obtained for different applied currents.*
- *A semi-active suspension system using the MR damper was quite successful in vibration mitigation.*

Graphical Abstract

In this study, an MR damper was designed, fabricated and its damping characteristics were experimentally investigated. Also, its equivalent damping coefficients were obtained and a suspension system with MR damper was simulated in Matlab/Simulink.

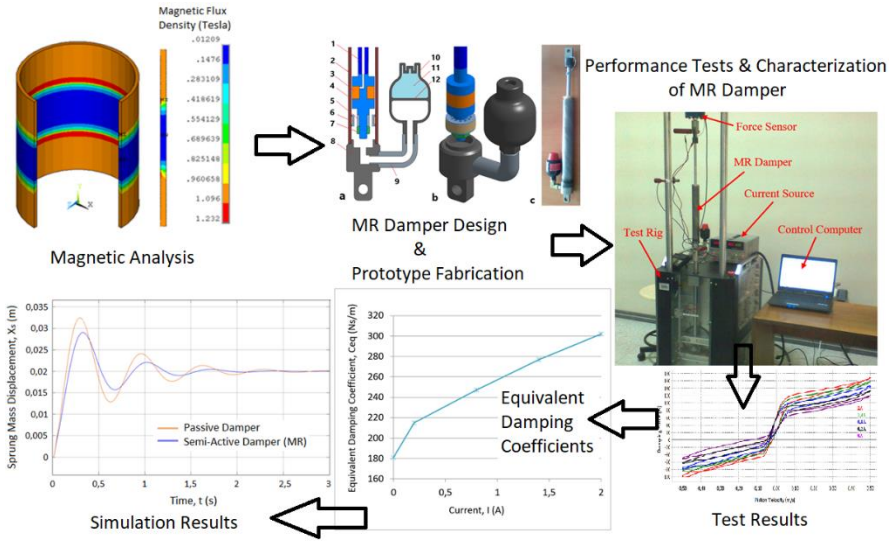

Figure. Graphical abstract

Aim

The aim of this study is to design, manufacture and characterize an innovative MR damper and to determine its effectiveness in vibration mitigation.

Design & Methodology

The MR damper was designed and prototyped according to the magnetic analysis. The damping performance was examined with the tests and equivalent damping coefficients were calculated according to the test results.

Originality

In this study, an innovative MR damper was designed and prototyped. The MR damper was filled with the MR fluid synthesized in previous studies and the damping characteristics were determined in the damper test device. In addition, the equivalent damping coefficients of the MR damper for different currents were obtained.

Findings

The highest damping force is 169.4 N with frequency of 3.18 Hz and applied current of 2 A. Also, the equivalent damping coefficients of the MR damper were ranging between 181 Ns/m and 302 Ns/m.

Conclusion

It was seen that the designed and tested MR damper can be used effectively in a semi-active suspension system.

Declaration of Ethical Standards

The author(s) of this article declare that the materials and methods used in this study do not require ethical committee permission and/or legal-special permission.

Experimental Study on Magnetorheological Damper Prototype and Obtaining Its Equivalent Damping Coefficients

Araştırma Makalesi / Research Article

Turgay ERGİN*, Duran ALTIPARMAK

Department of Automotive Engineering, Faculty of Technology, Gazi University, Ankara, Türkiye

(Geliş/Received : 24.02.2022 ; Kabul/Accepted : 06.04.2022 ; Erken Görünüm/Early View : 18.04.2022)

ABSTRACT

In this work, a magnetorheological (MR) damper prototype that provides controllable damping force was designed, manufactured and tested. The design and dimensions of the MR damper piston were determined according to the static magnetic analysis results made in ANSYS/Emag (Electromagnetics) software. The MR damper's damping performance was tested in laboratory by utilizing a damper testing device. The tests were carried out under different currents applied to coil of the MR damper. According to the test results, the equivalent damping coefficients of the MR damper were calculated for different currents. The test results show that the highest damping force is 169.4 N with frequency of 3.18 Hz and applied current of 2 A. In this case, the equivalent damping coefficient is 302 Ns/m. The equivalent damping coefficient is 181 Ns/m when no current is supplied to the coil. The area of the dynamic force range also becomes larger with increasing the applied current. In addition, according to the quarter car model based simulation results in MATLAB/Simulink, it was seen that the semi-active suspension system using MR damper was more effective and successful in vibration mitigation.

Keywords: Magnetorheological fluid, magnetorheological damper, equivalent damping, quarter car, magnetic analysis.

Manyetoreolojik Amortisör Prototipinin Deneysel Çalışması ve Eşdeğer Sönüm Katsayılarının Elde Edilmesi

ÖZ

Bu çalışmada, kontrol edilebilir sönümleme kuvveti sağlayan manyetoreolojik (MR) bir amortisör prototipi tasarlanmış, üretilmiş ve test edilmiştir. MR amortisör pistonunun tasarımı ve boyutları ANSYS/Emag (Elektromanyetik) yazılımında yapılan statik manyetik analiz sonuçlarına göre belirlenmiştir. MR amortisörün sönümleme performansı, bir amortisör test cihazı kullanılarak laboratuvarda test edilmiştir. Testler, MR amortisörün bobinine uygulanan farklı akımlar altında gerçekleştirilmiştir. Test sonuçlarına göre farklı akımlar için MR amortisörün eşdeğer sönüm katsayıları hesaplanmıştır. Test sonuçları, 3,18 Hz frekans ve uygulanan 2 A akım değeri için, en yüksek sönümleme kuvvetinin 169,4 N olduğunu göstermektedir. Bu durumda, eşdeğer sönümleme katsayısı 302 Ns/m'dir. Bobine akım verilmediğinde eşdeğer sönümleme katsayısı 181 Ns/m'dir. Dinamik kuvvet aralığının alanı da uygulanan akımın artmasıyla büyümüştür. Ayrıca MATLAB/Simulink'te çeyrek taşıt modeli tabanlı simülasyon sonuçlarına göre MR amortisör kullanan yarı aktif süspansiyon sisteminin titreşim azaltmada daha etkili ve başarılı olduğu görülmüştür.

Anahtar Kelimeler: Manyetoreolojik sıvı, manyetoreolojik amortisör, eşdeğer sönümleme, çeyrek taşıt, manyetik analiz.

1. INTRODUCTION

MR fluids are magnetic field dependent fluids. Viscosity of the MR fluids can be controlled by applying different magnetic fields to the damper coil. The viscosity of MR fluids increases as the magnetic field increases. MR fluids generally consist of magnetic particles dispersed in a carrier fluid [1]. Silicon oil is commonly used as carrier fluid and carbonyl iron particles are used as magnetic particles in MR fluids [1-4]. Silica is frequently used as an additive material to avoid the sedimentation problem [2-5]. MR fluids typically contain range of 20-80 wt% of carbonyl iron and range of 1-3 wt% of fumed silica in the literature [3,5].

Looking at the studies, MR fluids are used in automotive suspension [6-8], brake [9-11] and clutch [12,13] systems. There are many studies in the literature about its use, especially in semi-active suspension systems. Although active suspension system gives the best performance, it has some disadvantages such as more power requirement and expensive price. In contrast, semi-active suspension system needs less power and it is inexpensive. The studies on MR damper are mostly on novel damper designs [14-17] and controller designs [18-20].

*Sorumlu Yazar (Corresponding Author)
e-posta : turgayergin@gazi.edu.tr

In general, three principal operating modes are used in MR devices. These modes are referred to as shear, flow (valve) and squeeze mode. Also, mixed mode, which is a combination of these modes, is used. An MR damper has been designed and manufactured on the basis of mixed mode operation, which is a combination of flow and shear modes in a study [7]. A new design idea for the MR damper with a combination of squeeze and shear modes has been presented in an other study [21]. In addition, many studies involving different flow channel designs for MR dampers are available in the literature [14,17,22,23].

The damping force can be changed with the current applied to the damper coil. Since the damping coefficient of the MR damper can be controlled by the magnetic field, this provides an advantage in reducing vibrations. The wide range of damping force of the MR damper allows to exhibit different damping characteristics. The amount of energy absorbed by the MR damper in one full cycle is used to calculate the equivalent damping coefficient. The equivalent damping coefficients can be used for analyzing the effects of the MR damper on the quarter car model. [24]. The equivalent damping coefficients play an important role in the characterization of the MR damper. Therefore, the equivalent damping coefficients have been obtained in many studies [14,17,18].

The aim of this study is to design, manufacture and characterize an MR damper with limited radial dimensions. Radial dimensions are limited because the outer dimensions of a standard damper are used. Mixed mode, which is a combination of shear and valve mode, is used in the MR damper design. The inner structure and dimensions of the MR damper were determined according to a static magnetic analysis. Pre-synthesized MR fluid was used in the MR damper prototype. The properties of the MR fluid used are given in detail in the following of the study. The MR damper prototype was tested at constant frequency under harmonic excitation input. The damping performance curves of the MR damper were obtained. The amount of energy absorbed by the MR damper in one cycle was determined for different currents. The equivalent damping coefficients, which are the indicator of the damping performance of the MR damper, are also calculated. In addition, the quarter car models using passive and semi-active dampers were simulated in MATLAB/Simulink. The equivalent damping coefficients obtained were used in the quarter car model simulation for the semi-active suspension system equipped with the MR damper. The simulation results of passive and semi-active suspension systems were compared with each other in terms of vibration damping capabilities. Therefore, sprung mass responses were plotted as displacement and acceleration versus time.

2. MATERIAL and METHOD

The MR damper normally needs MR fluid for damping. The MR fluid was synthesized to be used in MR damper. The MR fluid was prepared with 40 %wt of carbonyl iron concentration by weight and silicone oil was used as carrier liquid. Also, 2 %wt of fumed silica was used as an additive to reduce sedimentation of the carbonyl iron particles [25]. All these materials were obtained from Sigma Aldrich. The properties of MR fluid and materials used in MR fluid synthesis are shown in Table 1.

Table 1. Properties of materials used in the MR fluid synthesis.

Parameter	Density (kg/m^3)	Particle Size (µm)	Iron Content (m/m, %)
Carbonyl iron	7860	4.5 - 5.2	≥ 97
Silicone oil	1000	-	-
Fumed silica	35.24	0.007	-
MR fluid	1510	-	-

The MR damper design was determined according to the static magnetic analysis results made in the ANSYS/Emag software. In this analysis, four different models with different MR fluid gaps were used. The MR fluid gaps used in the analysis are 0.5, 0.75, 1 and 1.25 mm. Since the MR fluid is predicted to reach magnetic saturation of around 1 T, the model with an MR fluid gap of 1 mm was chosen for the design. The magnetic flux density in the MR fluid gap for the current of 2 A is shown in Fig. 1. The magnetic flux density in the MR fluid layer around the damper piston is shown here. It is seen that the magnetic flux density in the effective MR fluid gap is around 1 T.

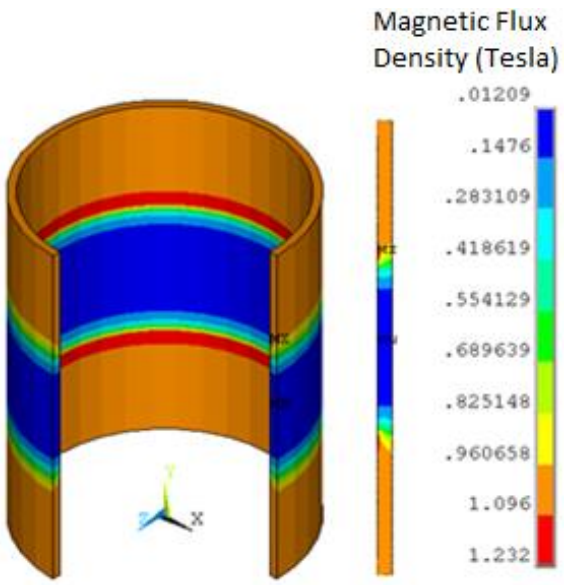

Fig. 1. The magnetic flux density in the MR fluid gap (gap is 1 mm).

Dimensions of the MR damper piston determined according to the static magnetic analysis are shown in Fig. 2. This 2D geometric model was created in the ANSYS/Emag software. Here, dimensions are in millimeter. The damper piston is seen as axisymmetric. The axisymmetric structure is widely used to simplify the magnetic analysis [11,14,15,22].

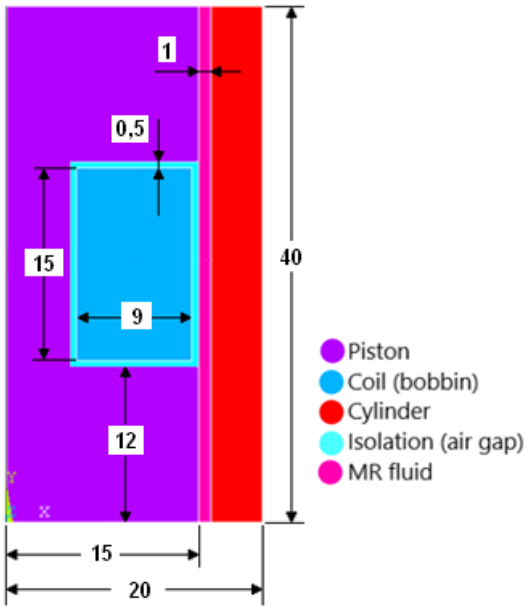

Fig. 2. Dimensions of the MR damper piston determined according to the static magnetic analysis results.

A prototype of the MR damper was designed and manufactured. Low carbon steel with high magnetic permeability was used as piston and cylinder material. A guide piston was used to center the damper piston in the cylinder. The material of the guide piston is aluminum so that it is not affected by the magnetic field. The coil has 702 turns of 0.4 mm diameter wire. The conductor used in the coil is enamel coated copper wire. Insulation material was used around the coil to prevent short circuit. The positive and negative terminals supplying the coil with current were passed through the piston rod of the damper. As the piston rod enters the cylinder during the compression stroke, a volume change occurs. Since liquids are considered incompressible, volume change must be tolerated. Therefore, a hydraulic accumulator was added to the MR damper prototype. The volume of the hydraulic accumulator is 0.05 lt and there is dry nitrogen gas at 10 bar pressure in it. The Fig. 3 shows the inner structure, main parts and prototype of the MR damper.

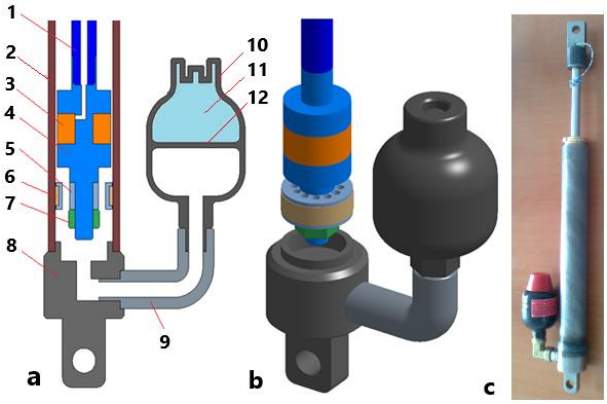

Fig. 3. Demonstration of the developed MR damper:

a) schematic diagram of inner structure, b) solid model of bottom of the MR damper, c) prototype of the MR damper

1: piston rod, 2: cylinder, 3: coil, 4:piston, 5: guide piston, 6: seal, 7: nut, 8: bottom cover, 9: hydraulic accumulator connector, 10: hydraulic accumulator, 11: dry nitrogen gas, 12: separator diaphragm

Designed and manufactured prototype of the MR damper is characterized using harmonic displacement input. The MR damper was excited at constant displacement amplitude of ±25 mm. Also, the tests were performed at constant frequency of 3.18 Hz. The tests were carried out at an ambient temperature of 20 °C. At the beginning of each test, the test device was operated at a speed of 0.2 m/s and for 10 s in an idle time to stabilize the MR damper. No data was collected during this process. The magnetic field in the coil was changed with the current adjusted to be between 0 A and 2 A. According to the magnetic analysis, the MR fluid in the MR fluid gap reached magnetic saturation by applying a current of 2A. For this reason, the current applied to the coil was chosen as maximum 2A. It is the magnetic field change that provides the damping force increase. The current source in the test setup was used to supply the coil with direct current (DC). The tests of the MR damper were performed on the damper test device in the Department of Mechanical Engineering at Hacettepe University. The test device can be completely controlled by a computer, thanks to its own software, SHOCKTM. This software is a test control and damper analysis software. The test device can measure the characteristics of the MR damper under various sinusoidal input frequencies. The experimental setup used for the tests is presented in Fig. 4.

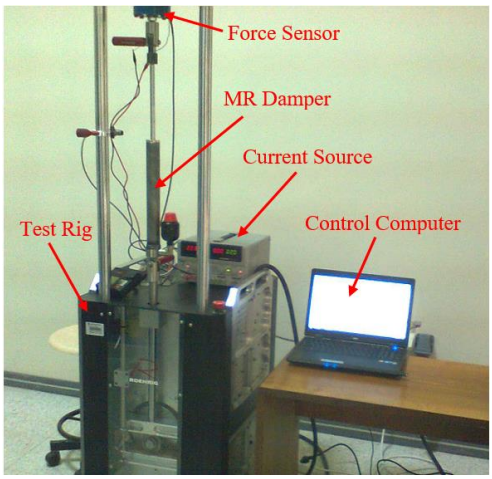

Fig. 4. Experimental setup for the MR damper.

3. RESULTS and DISCUSSION

A series of test is performed to measure characteristics of the MR damper under harmonic excitation. Damping force tests at relatively low velocities were performed on an electrically powered test rig to evaluate the damping characteristics of the MR damper prototype. Thus, the effectiveness of the MR damper was demonstrated. As shown in Fig. 5 and 6, the force – velocity F(V) and the force – displacement F(X) relationships are obtained directly from the tests. The tests were done both under sinusoidal excitation at a constant frequency of 3.18 Hz and at different currents applied to coil, that vary from 0 A (no current applied) to 2 A (maximum current applied). Here, the applied currents are 0.2, 0.8, 1.4 and 2.0 A, respectively.

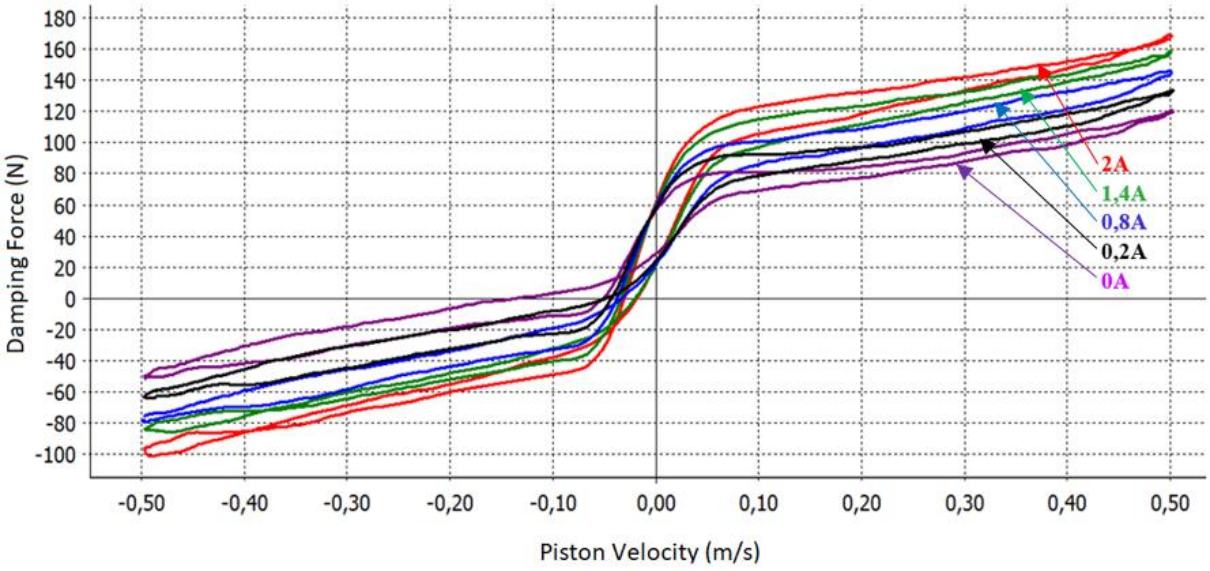

Fig. 5. Damping force vs. velocity loop (at constant frequency of 3.18 Hz).

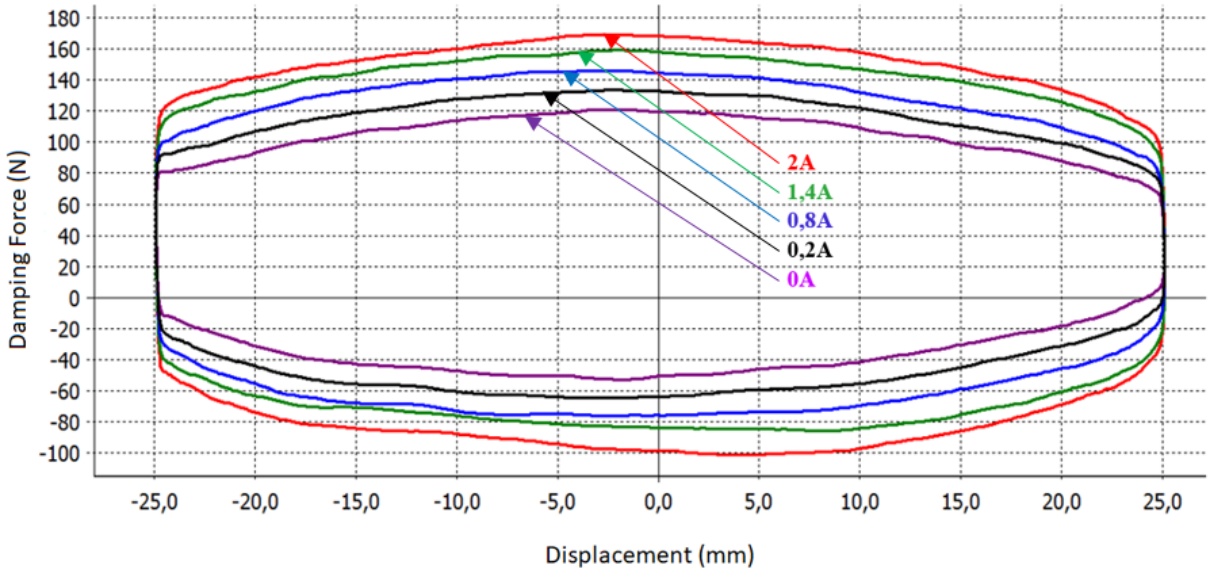

Fig. 6. Damping force vs. displacement loop (at constant frequency of 3.18 Hz).

When it comes to the cyclic characteristic, it is important that the shape of the loop F(X) be smooth. Basically, this indicates smooth valve characteristics and no cavitation within the normal operating range [26]. The F(X) loops of the MR damper designed is very smooth, as shown in Fig. 6. Also, it is observed that the areas of the F(X) loops increase with the increase of the applied current.

Figure 5 shows that as the piston velocity increases, the damping force also increases. The damping force increases as the applied current increases, and the area of the dynamic force range also becomes larger. The area seen in Fig. 7 is an indicator of the controllability of the MR damper. The larger area is the better controllability. Controllability of the MR damper allows adjustment of damping requirements for mitigating the undesirable vibration.

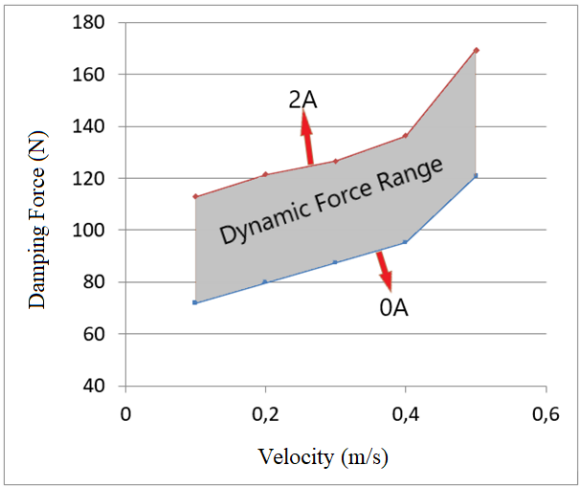

Fig. 7. Dynamic force range of the MR damper.

3.1. Obtaining The Equivalent Damping Coefficients

The area of the F(X) loop determines the amount of energy dissipated by the MR damper in one full cycle. The equivalent damping coefficient (ceq) of the MR damper for sinusoidal excitation can be calculated using Eq (1) [26]. Here, Ec is the energy dissipated by the damper in one cycle, X0 is the amplitude of the excitation displacement, and f is the frequency of sinusoidal excitation.

$$c_{eq} = \frac{E_c}{2\pi^2 f \ X_0^2} \quad (1)$$

The equivalent damping coefficients are obtained and plotted, as shown in Fig. 8. It can be deduced that the equivalent damping coefficient is ranging between 181 Ns/m and 302 Ns/m for different currents applied to the coil of the MR damper. It is clear that the equivalent damping coefficient increases with the increase of the current applied to the MR damper coil. When the current approaches 2 A, the magnetic circuit parts of the MR damper reaches to the saturation point. Therefore, the equivalent damping coefficient changes slowly.

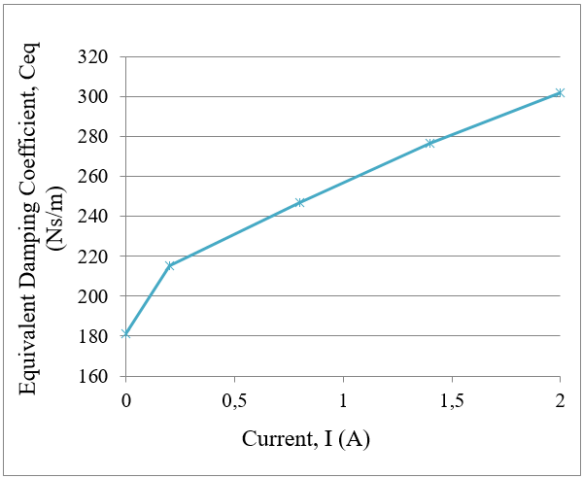

Fig. 8. Equivalent damping coefficients under different applied currents.

3.2. The Quarter Car Model Based Simulation

A quarter car model is one of the very known, simple and useful model to study vertical dynamics of a suspension system. The quarter car model consists of a sprung mass (ms), an unsprung mass (mus), a spring and a damper as shown in Fig. 9. Suspension spring stiffness (ks) and suspension damping coefficient (cs) are important parameters used in the quarter car model. Tire stiffness (kus) and tire damping coefficient (cus) have also been considered in this study. All these parameters used in the quarter car model are shown in Table 2.

Table 2. The parameters used in the quarter car model.

Parameter	Value
Sprung mass (m_s)	80 kg
Unsprung mass (m_{us})	8 kg
Suspension spring stiffness (k_s)	3000 N/m
Tire stiffness (k_{us})	30000 N/m
Suspension damping coefficient (c_s) [Passive/Semi-active (min-max)]	200/181-302 Ns/m
Tire damping coefficient (c_{us})	10 Ns/m

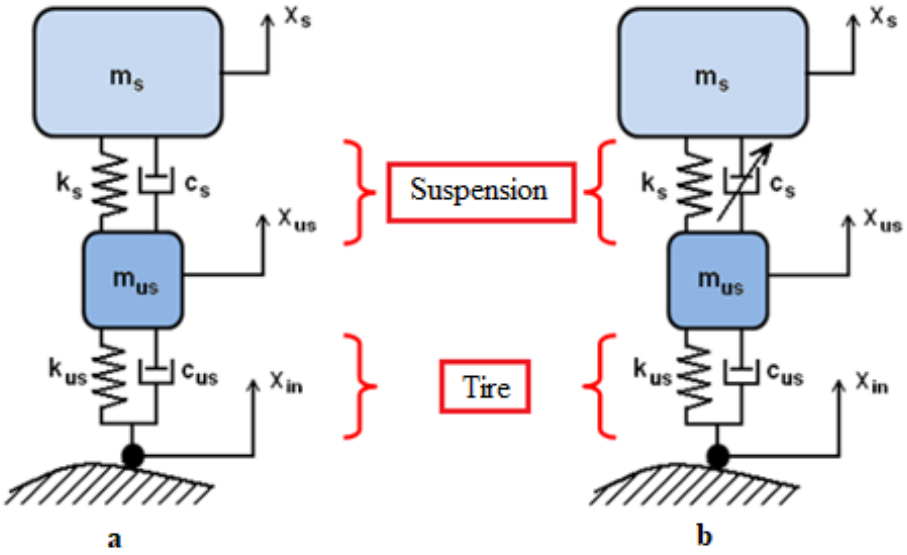

Fig. 9. Quarter car model for (a) passive and (b) semi-active suspension system.

In this study, two different quarter car models were created using passive and semi-active dampers. The quarter car models were simulated in MATLAB/Simulink. Step input excitation (xin) shown in Fig. 10 is used in both models. The step input excitation is 20 mm. The damping coefficients of the MR damper designed and manufactured are used in the semi-active model. In the semi-active suspension system, the switch (on/off) controller was used because it was useful and simple. The model works in this controller with two different damping coefficients as maximum (hard) and minimum (soft). Since the average constant damping coefficient was used in the passive model, no controller was used. The equations of motion for the quarter car model are given by Eq (2) and Eq (3). The operating conditions of the switch controller are given in Eq (4). Here, the purpose is to reduce vibration by reducing suspension forces.

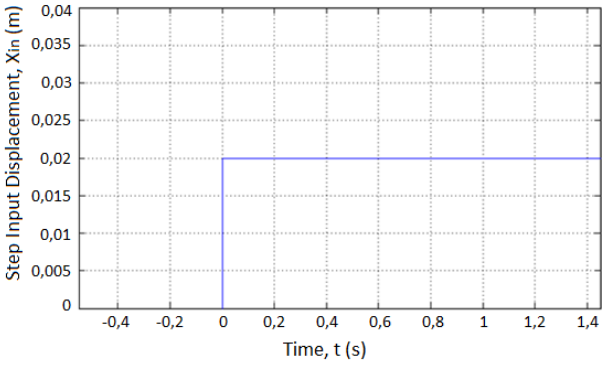

Fig. 10. Step input displacement vs. time for the quarter car models.

$$m_s\ddot{x}_s + c_s\left(\dot{x}_s - \dot{x}_{us}\right) + k_s\left(x_s - x_{us}\right) = 0 \tag{2}$$

$$m_{us}\ddot{x}_{us} + c_s\left(\dot{x}_{us} - \dot{x}_s\right) + k_s\left(x_{us} - x_s\right) + c_{us}\left(\dot{x}_{us} - \dot{x}_{in}\right) + k_{us}\left(x_{us} - x_{in}\right) = 0 \tag{3}$$

$$c_s(t) = \begin{cases} c_{s\min}, \left(x_s - x_{us}\right)\left(\dot{x}_s - \dot{x}_{us}\right) \geq 0 \\ c_{s\max}, \left(x_s - x_{us}\right)\left(\dot{x}_s - \dot{x}_{us}\right) < 0 \end{cases} \tag{4}$$

The simulation results comparing the passive and the semi-active systems are shown in Fig. 11 and 12. The sprung mass response is given as displacement and acceleration versus time for both models. Sprung mass displacement of the semi-active system is less than the passive system. In addition, body oscillations are damped in a shorter time in the semi-active system. Also, sprung mass acceleration of the semi-active system is lower than the passive system. According to the simulation results, it is clear that the semi-active system gives better results in vibration reduction than the passive system.

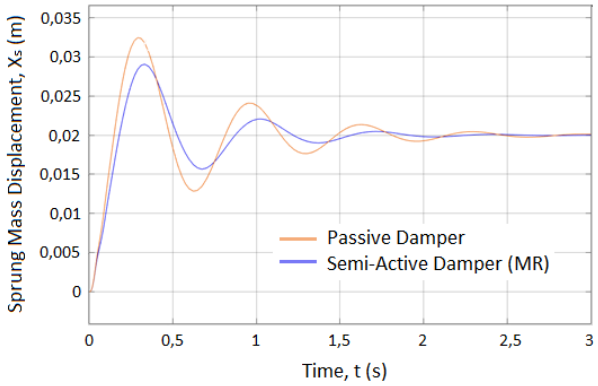

Fig. 11. Sprung mass displacement vs. time for the quarter car models.

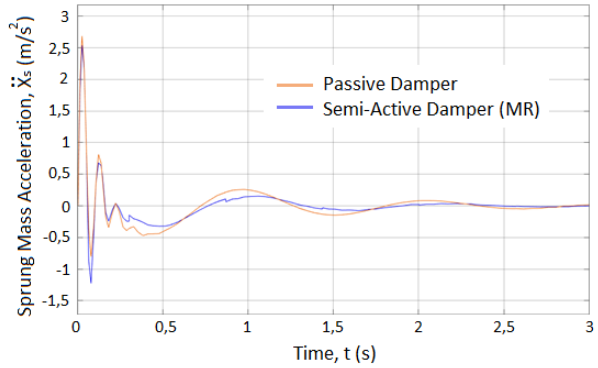

Fig. 12. Sprung mass acceleration vs. time for the quarter car models.

4. CONCLUSIONS

It is clearly seen that the damping force increases with the increase of the applied current. The applied current has a significant effect on the damping force of the MR damper. When applied current reaches to 2 A, the maximum damping force is measured as 169.4 N. The dynamic force range, which indicates the controllable force range, increased with the increase of the magnetic field. Therefore, the amount of energy absorbed by the MR damper was also increased. Controllability of the MR damper allows damping requirements to be adjusted very quickly.

The equivalent damping coefficients of the MR damper were found to vary between 181 Ns/m and 302 Ns/m. These results show that the MR damper has a very high vibration control capability. Up to 66.8% increase occurred in the equivalent damping coefficient. These damping coefficients were used in the quarter car model simulation in MATLAB/Simulink. The simulation results showed that the semi-active suspension system using the MR damper was more successful than the passive system in vibration mitigation.

ACKNOWLEDGEMENT

This work was supported by Gazi University Scientific Research Projects Unit. Project Number: 07/2010-29, 2010.

DECLARATION OF ETHICAL STANDARDS

The author(s) of this article declare that the materials and methods used in this study do not require ethical committee permission and/or legal-special permission.

AUTHORS' CONTRIBUTIONS

Turgay Ergin: Performed the experiments, analysed the results and wrote the manuscript.

Duran Altıparmak: Analysed the results and edited the manuscript.

CONFLICT OF INTEREST

There is no conflict of interest in this study.

REFERENCES

[1] G. Bossis, S. Lacis, A. Meunier, O. Volkova, "Magnetorheological fluids", ***Journal of Magnetism and Magnetic Materials,*** 252: 224-228, (2002).

[2] Y. D. Liu, F. F. Fang, H. J. Choi, "Core-shell-structured silica-coated magnetic carbonyl iron microbead and its magnetorheology with anti-acidic characteristics", ***Colloid Polym Sci.,*** 289: 1295-1298, (2011).

[3] M. Kciuk, S. Kciuk, R. Turczyn, "Magnetorheological characterisation of carbonyl iron based suspension", ***Journal of Achievements in Materials and Manufacturing Engineering,*** 33: (2) 135-141, (2009).

[4] P. B. Nguyen, X. P. Do, J. Jeon, S. B. Choi, Y. D. Liu, H. J. Choi, "Brake performance of core-shell structured carbonyl iron/silica based magnetorheological suspension", ***Journal of Magnetism and Magnetic Materials,*** 367: 69-74, (2014).

[5] M. N. Aruna, M. R. Rahman, S. Joladarashi, H. Kumar, B. P. Devadas, "Influence of different fumed silica as thixotropic additive on carbonyl particles magnetorheological fluids for sedimentation effects", ***Journal of Magnetism and Magnetic Materials,*** 529: 167910, (2021).

[6] H. Pang, F. Liu, Z. Xu, "Variable universe fuzzy control for vehicle semi-active suspension system with MR damper combining fuzzy neural network and particle swarm optimization", ***Neurocomputing,*** 306: 130-140, (2018).

[7] M. Yu, X. M. Dong, S. B. Choi, C. R. Liao, "Human simulated intelligent control of vehicle suspension system with MR dampers", ***Journal of Sound and Vibration,*** 319: 753-767, (2009).

[8] J. Yang, D. Ning, S. S. Sun, J. Zheng, H. Lu, M. Nakano, S. Zhang, H. Du, W. H. Li, "A semi-active suspension using a magnetorheological damper with nonlinear negative-stiffness component", ***Mechanical Systems and Signal Processing,*** 147: 107071, (2021).

[9] S. Acharya, R. S. Saini Tak, S. B. Singh, H. Kumar, "Characterization of magnetorheological brake utilizing synthesized and commercial fluids", ***Materials Today: Proceedings***, https://doi.org/10.1016/j.matpr.2020.03.061 , (2020).

[10] S. M. Kalikate, S. R. Patil, S. M. Sawant, "Simulation-based estimation of an automotive magnetorheological

brake system performance", ***Journal of Advanced Research,*** 14: 43-51, (2018).

[11] E. J. Park, D. Stoikov, L. F. Luz, A. Süleman, "A performance evaluation of an automotive magnetorheological brake design with a sliding mode controller", ***Mechatronics***, 16: 405-416, (2006).

[12] K. H. Latha, P. U. Sri, N. Seetharamaiah, "Design and Manufacturing Aspects of Magneto-rheological Fluid (MRF) Clutch", ***Materials Today: Proceedings***, 4: 1525-1534, (2017).

[13] J. Y. Park, G. W. Kim, J. S. Oh, Y. C. Kim, "Hybrid multi-plate magnetorheological clutch featuring two operating modes: Fluid coupling and mechanical friction", ***Journal of Intelligent Material Systems and Structures***, 1-13, https://doi.org/10.1177/1045389X20988086 , (2021).

[14] X. X. Bai, D. H. Wang, H. Fu, "Principle, modeling, and testing of an annular-radial-duct magnetorheological damper", ***Sensors and Actuators A: Physical,*** 201: 302-309, (2013).

[15] F. Tu, Q. Yang, C. He, L. Wang, "Experimental Study and Design on Automobile Suspension Made of Magneto-Rheological Damper", ***Energy Procedia***, 16: 417-425, (2012).

[16] G. Hu, Y. Lu, S. Sun, W. Li, "Development of a self-sensing magnetorheological damper with magnets in-line coil mechanism", ***Sensors and Actuators A: Physical,*** 255: 71-78, (2017).

[17] M. Mao, W. Hu, Y. T. Choi, N. M. Wereley, "A magnetorheological damper with bifold valves for shock and vibration mitigation", ***Journal of Intelligent Material Systems and Structures***, 18: 1227-1232, (2007).

[18] G. Z. Yao, F. F. Yap, G. Chen, W. H. Li, S. H. Yeo, "MR damper and its application for semi-active control of vehicle suspension system", ***Mechatronics***, 12: 963-973, (2002).

[19] R. Jeyasenthil, S. B. Choi, "A novel semi-active control strategy based on the quantitative feedback theory for a vehicle suspension system with magneto-rheological damper saturation", ***Mechatronics,*** 54: 36-51, (2018).

[20] J. Wu, H. Zhou, Z. Liu, M. Gu, "A load-dependent PWA-H∞ controller for semi-active suspensions to exploit the performance of MR dampers", ***Mechanical Systems and Signal Processing,*** 127: 441-462, (2019).

[21] I. I. M. Yazid, S. A. Mazlan, T. Kikuchi, H. Zamzuri, F. Imaduddin, "Design of magnetorheological damper with a combination of shear and squeeze modes", ***Materials and Design,*** 54: 87-95, (2014).

[22] G. Hu, H. Liu, J. Duan, L. Yu, "Damping performance analysis of magnetorheological damper with serial-type flow channels", ***Advances in Mechanical Engineering,*** 11: (1) https://doi.org/10.1177/1687814018816842 , (2019).

[23] I. Bahiuddin, F. Imaduddin, S. A. Mazlan, M. H. M. Ariff, K. B. Mohmad, Ubaidillah, S. B. Choi, "Accurate and fast estimation for field-dependent nonlinear damping force of meandering valve-based magnetorheological damper using extreme learning machine method", ***Sensors and Actuators A: Physical,*** 318: 1-12, https://doi.org/10.1016/j.sna.2020.112479 , (2021).

[24] M. H. Jamadar, R. M. Desai, H. Kumar, S. Joladarashi, "Analyzing quarter car model with magneto-rheological (MR) damper using equivalent damping and magic formula models", ***Materials Today: Proceedings***, 1-6, https://doi.org/10.1016/j.matpr.2021.02.706 , (2021).

[25] T. Ergin, D. Altıparmak, "Damping performance of carbonyl iron and magnetite-based magnetorheological fluids and usage of fumed silica as an additive", ***Journal of the Faculty of Engineering and Architecture of Gazi University,*** 28: (4) 695-703, (2013).

[26] J. C. Dixon, "The Shock Absorber Handbook", ***John Wiley & Sons Ltd.***, Chp-7, England, (2007).